We are IntechOpen,
the world's leading publisher of
Open Access books
Built by scientists, for scientists

4,800
Open access books available

122,000
International authors and editors

135M
Downloads

154
Countries delivered to

Our authors are among the

TOP 1%
most cited scientists

12.2%
Contributors from top 500 universities

BOOK CITATION INDEX
CLARIVATE ANALYTICS
INDEXED

WEB OF SCIENCE™

Selection of our books indexed in the Book Citation Index
in Web of Science™ Core Collection (BKCI)

Interested in publishing with us?
Contact book.department@intechopen.com

Numbers displayed above are based on latest data collected.
For more information visit www.intechopen.com

Energy Dissipation Capacity in MWCNTs Reinforced Metal Matrix Nanocomposites: An Overview of Experimental Procedure

S. Ziaei-Rad, F. Karimzadeh, J. Kadkhodapour and M. Jafari
Isfahan University of Technology,
Iran

1. Introduction

Adsorption of vibration energy by mechanical damping is a significant problem in many engineering designs. High damping materials are used to reduce vibration in aircraft and other machinery. The benefits of damping treatment are advanced durability, reliability and service life of components, reductions in weight, noise and costs (Chung, 2001).

By invoking the properties of nanostructures it may be possible to control the shock wave propagation in the material and thus, significantly enhance the impact energy dissipation; however, only limited research papers concern about damping composite structures and shock resistant of nanomaterials.

If one goes to the nanoscale, the damping levels/dynamics of structures are mostly unknown and require extensive investigations. This chapter traces the experimental and analytical investigation methods for damping capacity and its application to nanocomposites.

A couple of works were published about investigation of damping capacity in different material (Koizumi et al., 2003; Gu et al., 2004; Srikanth & Gupta, 2005; Zhang et al, 2005; Botelhoa, 2006; Kireitseu et al., 2007; Yadollahpour et al., 2009). These works were summarized in Table 1. The first part of this chapter deals with an overview of experimental procedures for investigation of energy dissipation capacity in materials.

Carbon nanotubes (CNTs) have superior mechanical properties with an elastic modulus up to 1 TPa and a tensile strength up to 150 GPa and, as well as excellent thermal stability and electrical conductivity (Ci et al., 2006). Their exceptional mechanical properties make CNTs ideal candidates as reinforcements in composite materials to increase both stiffness and strength, while contributing to weight savings (Esawi & Morsi, 2007). Larger portion of the researches have been focused on the development of CNT reinforced polymer, ceramic based composites, and only a few studies have been concerned with the manufacture of CNT reinforced metal matrix composite (George et al., 2005;Chunfeng et al., 2007). It has been confirmed that the mechanical properties of metal matrix composites were improved, when an appropriate amount of nanotubes were added (Deng et al., 2007a). Beside considerable reinforcement effect of CNTs, fabrication of MMCs with nanostructured matrices may also provide excessive properties due to their greater mechanical characteristics compared to coarse-grained counterparts.

Table 1. Works on damping capacity of materials

Author	Year of publication	Material	
Y. Koizumi et al.	2003	ultra-fine grained aluminum produced by ARB	t
Z. Zhang et al.	2005	AZ91D magnesium alloy	I
M. Kireitseu et al.	2007	carbon nanotube-reinforced UHMW-PE polymer composite	
E.C. Botelho et al.	2006	Fiber–metal laminate (FML) composites	
J. Gu et al.	2004	aluminum matrix composites reinforced with coated carbon fibers	
N. Srikanth et al.	2005	aluminium based composites Ti particulates as reinforcement	
M. Yadollahpour et al.	2009	Al–Zn/α-Al2O3 of nanocomposite	

2. Experimental measurement methods for damping capacity

As shown in any vibrations textbook, the parameters describing the vibration response of a single degree of freedom (SDOF) spring-mass-damper system may be used in reporting damping test results (Thomson, 1972). Single degree of freedom damping parameters may be estimated by curve fitting to the measured response of material specimens in either free vibration or forced vibration if a single mode can be isolated for the analysis. Approximate

relationships between the loss factor from complex modulus notation and these SDOF damping parameters exist for lightly damped systems, (Soovere & Drake, 1985) and such relationships will be used frequently in the following subsections.

2.1 Free vibration methods

Observations of the free vibration response of a damped system are often used to characterize the damping in the system. If the specimen is released from some initial static displacement or if a steady-state forcing function is suddenly removed, the resulting free vibration response (Fig. 1a) may be analyzed using the logarithmic decrement, a SDOF damping parameter. The logarithmic decrement is given in Eq. (1)

$$\Delta = \frac{1}{n} \ln \frac{x_0}{x_n} \tag{1}$$

Where x_0 and x_n are amplitudes measured n cycles apart. Eq. (2) is based on the assumption of viscous damping, but for small damping, the loss factor from complex modulus notation may be approximated by Eq. (2) (Soovere & Drake, 1985).

$$Q^{-1} = \frac{\Delta}{\pi} \tag{2}$$

Commonly used modes of testing include torsional pendulum oscillation, and flexural vibration of beams or reeds. Errors may result if more than one mode of vibration is significant in the free vibration response, or if the data are taken at large amplitudes where air damping is present.
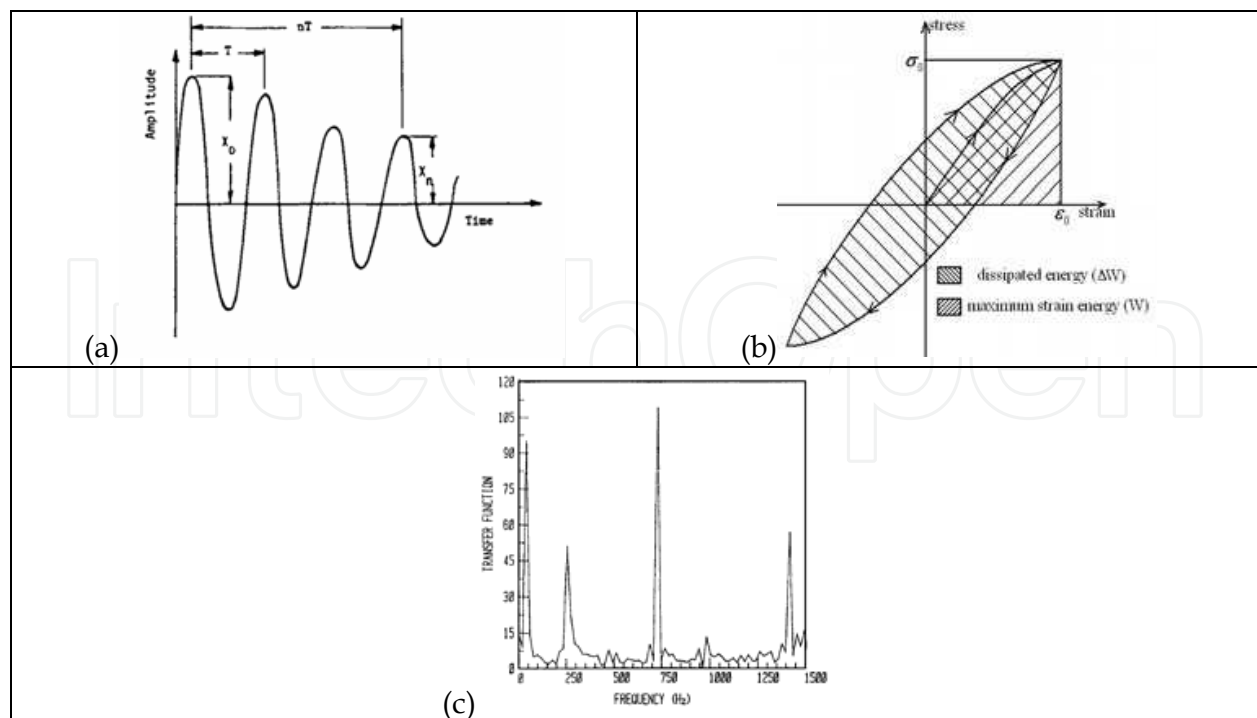

Fig. 1. (a) Free vibration decay curve (b) stress-strain hysteresis loop (c) typical frequency response curve

2.2 Forced vibration methods

Forced vibration techniques are often more useful than free vibration techniques when control of amplitude and frequency is desired. Excitation may be sinusoidal, random, or impulsive, and response may be analyzed in either the time domain or the frequency domain.

The simplest forced vibration technique involves the measurement of uniaxial hysteresis loops during low-frequency sinusoidal oscillation of a tensile specimen in a servohydraulic mechanical testing machine. The elliptical hysteresis loops are the Lissajous patterns formed by plotting the sinusoidally varying load (or stress) versus the corresponding strain (Fig. 1b). The energy dissipation ability of the composite material is evaluated by the ratio of the dissipated work by the material (ΔW) to the maximum of elastic energy stored in the cyclic loading process (W), and we use ψ to represent the ratio in Eq. (3) and the loss factor (Q-1) can be calculated from Eq. (4).

$$\psi = \frac{\Delta W}{W}$$
(3)

and

$$Q^{-1} = \frac{\psi}{2\pi}$$
(4)

With the forced vibration techniques discussed above, data are obtained at the frequency of oscillation of the exciter in the testing machine, which may or may not be a resonant frequency of the specimen. If the forcing frequency is tuned to a resonant frequency of the specimen, the relationship between the input and the response takes on a special form--this is the basis of the so-called resonant dwell method (Granick & Stem, 1965).

By varying the forcing frequency, the so-called frequency response curve (or response spectrum) for the specimen can be swept out in the frequency domain, as shown in Fig. 1c. The peaks in the curve represent resonant frequencies, and SDOF curve fitting techniques such as the half-power bandwidth can be used at these frequencies (Thomson, 1972, Soovere & Drake, 1985). The loss factor here is equal to:

$$Q^{-1} = \frac{\omega_2 - \omega_1}{\omega_n}$$
(5)

Where 1/Q is the damping factor and ωn is the peak frequency in the response curves (natural frequency). Parameters $\omega 1$ and $\omega 2$ are referred to as half-power points which are measured at $1/\sqrt{2}$ of peak amplitude.

3. Material preparation and characterization

Al2024 is one of the most widely used Al alloys in aerospace and automobile industries due to their high strength and specific stiffness. To prepare nanostructured Al2024 matrix, Al–4.1 wt.%; Cu–1.9 wt.%; Mg–0.5%Si (Al2024) prealloyed powder was milled in a planetary ball mill (Fritsch P7 type) under argon atmosphere. The milling media consisted of five 20mm diameter balls confined in a 120 ml volume vial. Ball milling was carried out with ball-powder mass ratio of 10:1 and rotation speed of 500 rpm for 30h. 0.5 wt.%. Stearic acid [$CH_3(CH_2)_{16}COOH$] was used as process control agent (PCA). Scanning electron

microscopy (SEM-Philips XL30) was used in order to evaluate the morphology changes of Al2024 powder particles through the ball milling process for 30h.

Multi-wall carbon nanotubes (MWCNTs) (provided by Research Institute of Petroleum Industry) were produced using catalytic chemical vapor deposition (CCVD) technique with purity of ~90%. To eliminate the catalyst particles and to disperse MWCNTs, they were immersed in concentrated nitric acid for 12h. MWCNTs were then washed with distilled water and dried at 120˚C. MWCNTs sample were characterized by transmission electronic microscope (TEM) (Philips CM12). After that, MWCNTs were added to the ethanol and dispersed using an ultrasonic shaker for 1h in order to maintain uniform distribution. Then, as-milled Al2024 powders were added to the MWCNTs–ethanol solution and the mixture was dispersed using ultrasonic shaker for another 30min. Subsequently, the mixed powders were dried at 120˚C in vacuum (~10-2Pa). In order to improve the dispersion of MWCNTs in the nanocomposite powders, ball milling was executed on nanocomposite powders for 4h. In this study, 1, 3 and 5 volume percent of MWCNTs were mixed with 30milled-Al2024 powders. Morphology of nanocomposite powder particles was then examined by SEM.

Final Al2024-MWCNT nanocomposite powders were compacted at 500˚C under 250MPa in a uniaxial die and then cooled in air, in order to produce disks with the size of ø50×10mm. The duration of hot pressing was 30 min.

The XRD patterns of as-received Al2024 powders, 30h-milled Al2024 powders and consolidated Al2024-MWCNTs nanocomposite samples were recorded using a Philips diffractometer with Cu Kα radiation (λ =0.15406 nm). The Al grain size in as-milled Al2024 and consolidated Al2024-3vol% MWCNTs samples were estimated from broadening of XRD peaks using Williamson-Hall formula (Williamson & Hall, 1953). Hardness tests were conducted on bulk nanocomposites at a load of 10 kg. The Archimedes technique was used to measure the bulk density of consolidated samples.
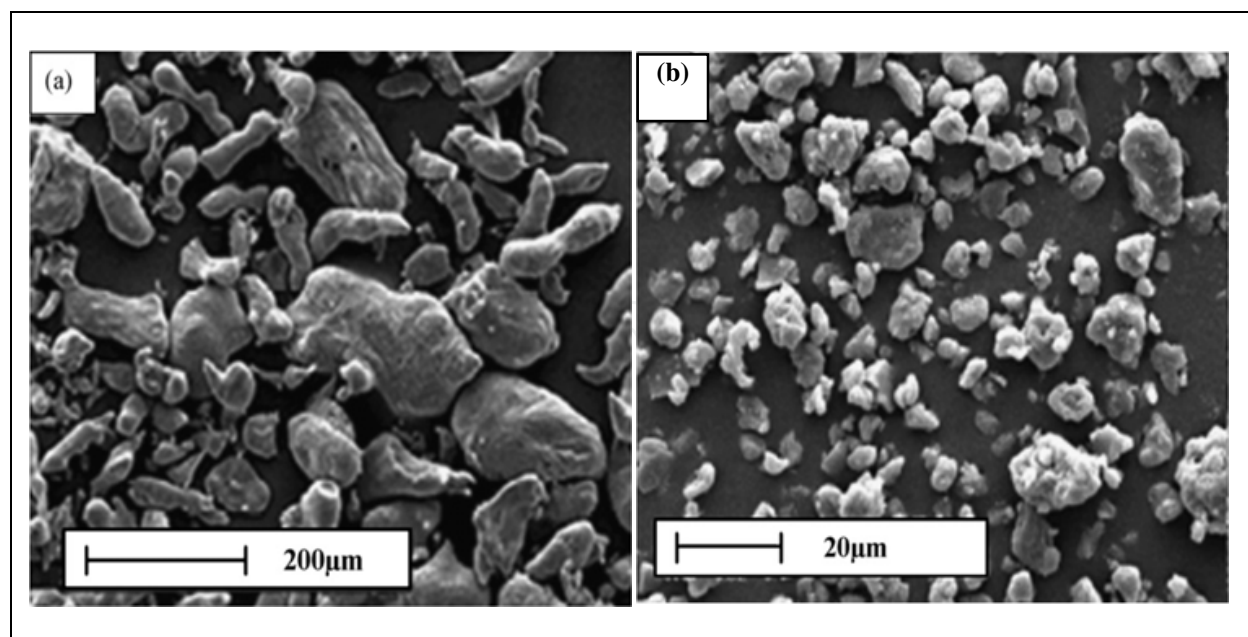

Fig. 2. a) As-received Al2024 powder b) 30h-milled Al2024 powder morphology

As-received Al2024 powder particles (see Fig. 2a) were irregular in shape and had non-uniform size ranging from 50 to 300μm. According to Fig. 1b, after 30h most powder particles were equiaxed with an average size of ~10μm. This decrease in powder particle

size is a consequent of stearic acid which diminishes cold welding of powders as well as work hardening effects of Al2024 powders during milling (Jafari et al., 2009).

Fig. 3a shows a TEM image of the purified carbon nanotubes. According to Fig. 3a, it can be found that the MWCNTs have outer diameters of 30 to 40nm and large aspect ratio. Also, it is evident that most MWCNTs enwind with each other, which apparently has a negative effect on dispersing them in the composites. In order to improve the dispersion of MWCNTs in the matrix, the Al2024-MWCNTs nanocomposite powders were mechanically milled for 4h. The SEM image of the nanocomposote powder after milling is shown in Fig. 3b. It is evident that the MWCNTs have been shortened so that the length of most of them has become less than 1μm.
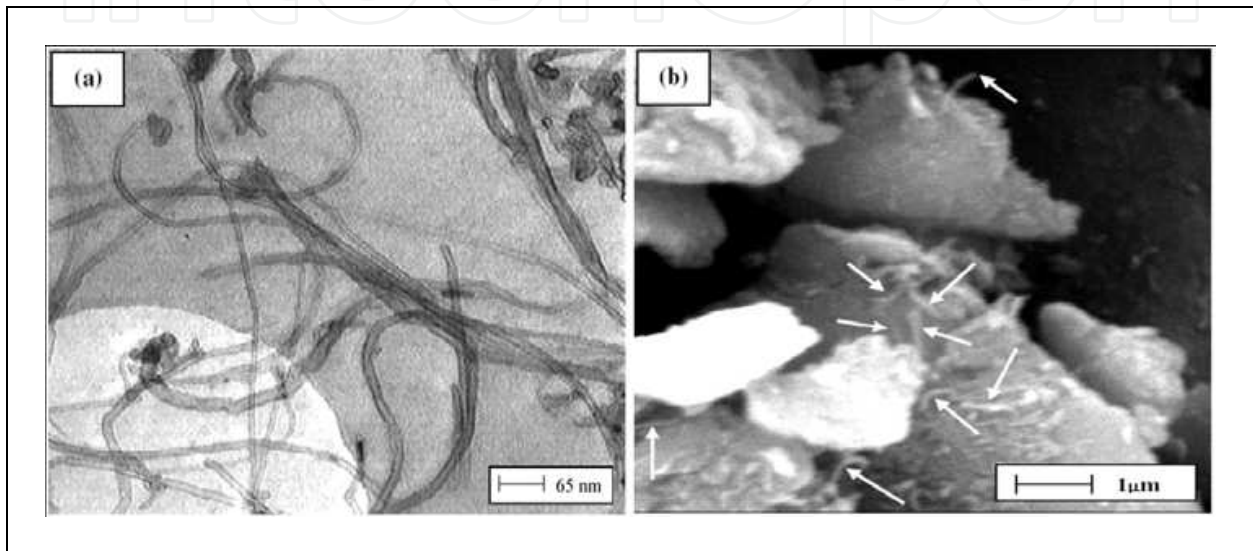
Fig. 3. a) TEM image of purified MWCNTs b) SEM micrograph of 4h-milled Al2024-3%vol MWCNT nanocomposite powders

The XRD patterns of as-received Al2024 powders, 30h-milled Al2024 powders and consolidated Al2024-MWCNTs nanocomposite samples are demonstrated in Fig. 4.
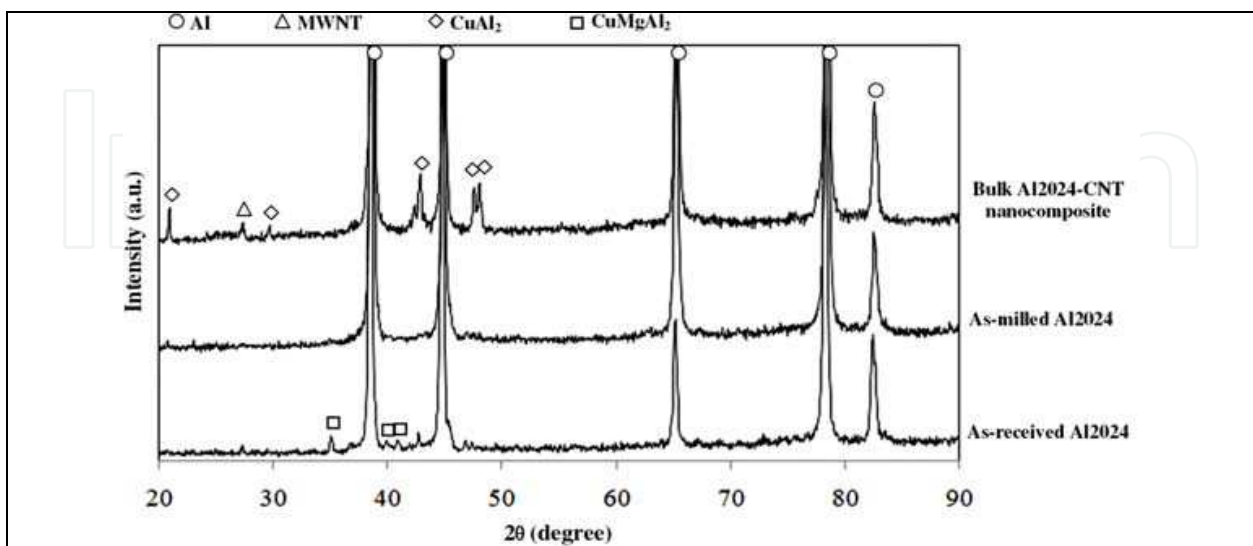

Fig. 4. XRD patterns of as-received Al2024 powders, 30h-milled Al2024 powders and bulk Al2024-3vol%MWCNTs nanocomposite

According to Fig. 4, the structure of as-received powder includes CuAl2 and CuMgAl2 intermetallic compounds. After 30h of ball milling, the intermetallic peaks completely disappeared on XRD patterns owing to the dissolution of CuAl2 and CuMgAl2 intermetallic compounds in Al lattice as well as grain boundaries (Jafari et al., 2009). It can also be assumed that these intermetallic compounds are dispersed into the Al as ultrafine isolated particles which are virtually undetectable by XRD (Tavoosi et al., 2008).

The Al grain size of 30h-milled Al2024 was estimated from broadening of XRD peaks using Williamson-Hall formula (Williamson & Hall, 1953). Due to the mechanical deformation introduced into the powders, Al grains refine so that after 30h of ball milling, Al grain size reaches a value of ~30nm.

XRD pattern of hot-pressed Al2024-3vol%MWCNT includes MWCNT (002) XRD peak appeared at 26.2° in the 2è value, indicating the presence of MWCNTs in the compound. Several peaks of CuAl2 intermetallic compound can be found in nanocomposite XRD pattern. The Al grain size in bulk Al2024-MWCNT was estimated ~42nm, using Williamson-Hall formula (Williamson & Hall, 1953).

4. Modal testing and analysis

The damping factor of the specimen was determined by use of modal testing (DTA, 1993, 2000; Ewins, 2001). The measurement principle consists of recording the free vibrations of the specimen excited by tapping it with an appropriate hammer, as shown in Fig. 5. The amplitude decay as a function of time and the vibration modes were detected by an acquisition data system from B&K Company and recorded using ICATS software (ICATS, 2003) and also by analytical relations.

The test specimen was located on soft foam and tested in a free-free condition. The experimental data were obtained via hammer testing using a B&K Pulse analyzer connected to a PC. One B&K piezoelectric accelerometer (Endevco. 2222c) was attached to the structure by using wax to measure the amplitude decay of the response (Fig. 5).The test parameters were: analyses range of 0-20,000 Hz; acquisition time of 320 ms; rectangular observation window and frequency resolution of 3.125 Hz. Following the testing procedure, two types of curves were obtained: damping free vibration and frequency response function profiles.
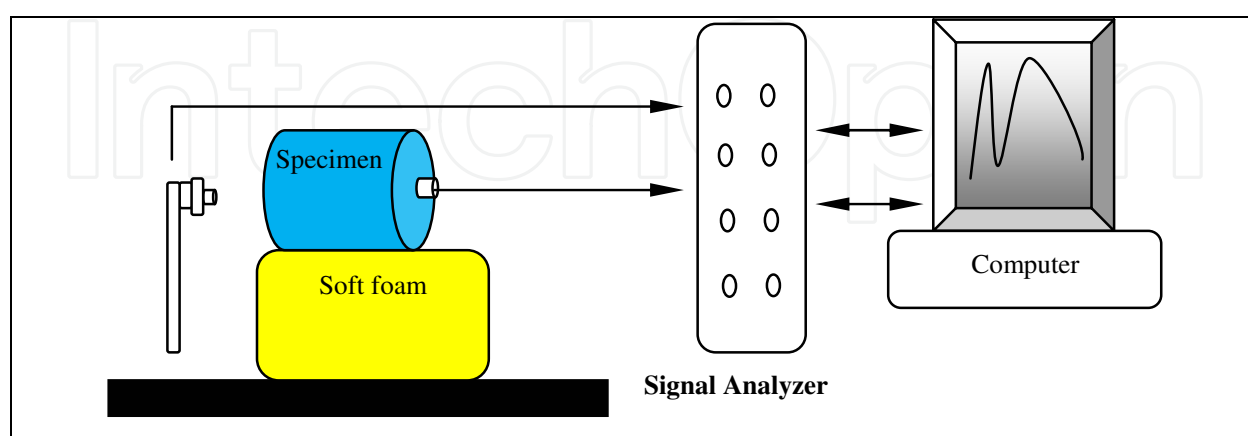

Fig. 5. The experimental set-up for modal testing of the specimen

The vibration test gives the free vibration damping decay and the frequency response function (FRF), simultaneously as a result. Considering a linear system of a single degree of

freedom, the FRF response is the decomposition of the natural frequencies of a structure or specimen, which corresponds to a typical fingerprint identity of the vibration modes. The number of vibration peak frequencies (vibration modes) and the shape of the FRF response are a direct result of the material damping.

In the second stage, the experimental FRF data were analyzed using a global multi-FRF analysis method and the results were also checked using available analytical relations. The global multi-FRF technique is based on a complex singular value decomposition of a system matrix expressed in terms of measured FRFs, and then on a complex eigensolution which extracts the required modal properties (Imregun & Ewins, 1995; ICATS, 2003). The data were analyzed by applying 3 runs on each FRF. Typical measured FRF is plotted in Fig. 6.

5. Results and discussion

The values of hardness and bulk density of Al2024 containing 1, 3 and 5vol% MWCNTs are summarized in Table 2.

Considering the data given in Table 2, it can be concluded that with small amounts of MWCNTs addition (less than 3vol. %), the relative density of the composites remains at approximately identical value of ~98%, mainly due to the uniform dispersion of MWCNTs within the Al2024 particles. Consequently, hardness of the composites increases with increasing MWCNTs content. However, large amounts of MWCNTs (~5vol. %) reduce the relative density and hardness of the composites, since MWCNTs tend to tangle together which results in preventing the appropriate densification of the specimens (Deng et al., 2007b).

Material	Relative density (Standard deviation of 0.5%)	Hardness (HV)
Al2024-1vol%MWCNT	98	220±5
Al2024-3vol%MWCNT	97.5	238±4
Al2024-5vol%MWCNT	93.5	195±6

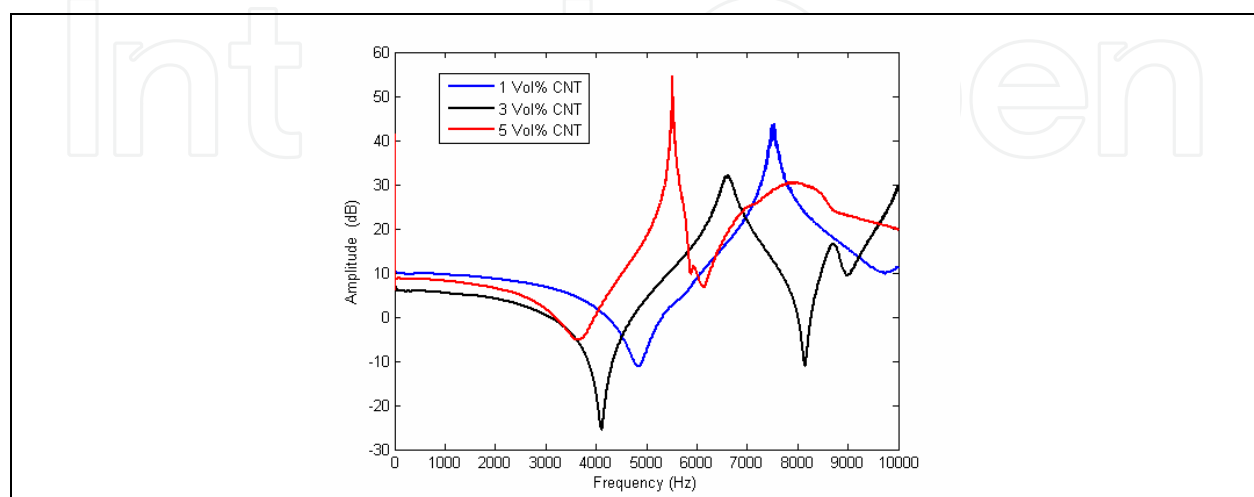Table 2. Hardness and bulk density values of Al2024-MWCNTs nanocomposites

Fig. 6. Measured frequency response function from excitation of the specimens

The damping capacity was also measured and the results of FRF test are presented in Fig 6. Natural frequency and damping factor are tabulated in Table 3. It comes out true that the natural frequency decreases as the volume percent of MWCNTs reinforcement increases. For damping factor, the trend is the same as hardness value to some extent. In other words, the damping factor increases as the MWCNTs volume percent increase from 1vol. % to 3vol. %. But further increase to 5vol. % causes reduction in damping factor. This phenomenon can be explained in the following way that the MWCNTs reinforcement causes increase in damping capacity but in 5vol. % specimen the cavity content play a more important role and cause reduction in damping factor.

FRF	Natural Frequency (HZ)	Damping factor (Eq. 20)	Damping factor ICATS (LINE FIT TECHNIQUE)
(1% vol CNT)	7302	0.031	.035
(3% vol CNT)	6268	0.052	0.057
(5% vol CNT)	5464	0.0105	.012

Table 3. Natural frequency and damping factor of Al2024-MWCNTs nanocomposites

6. Conclusion

Using a free vibration damping set up, the damping capacity of MWCNTs reinforced metal matrix nanocomposites was measured. It was observed that the damping capacity increases by increasing the vol% of the reinforcement. But as an undesirable feature of production process, increasing the vol% of reinforcement to 5 vol% causes a relatively large amount of porosity in the material which reduces the damping capacity.

7. References

Botelhoa, E.C.; Campos, A.N.; de Barros, E.; Pardini, L.C. & Rezende, L.C. (2006). Damping behavior of continuous fiber/metal composite materials by the free vibration method. *Composites: Part B,* Vol.37, pp. 255-266, ISSN 1359-8368

Chunfeng, D.; Xuexi, Z. & Dezun, W. (2007). Chemical stability of carbon nanotubes in the 2024Al matrix. *Materials Letters,* Vol.61, pp. 904-907, ISSN 0167-577X

Chung, TR. (2001). Materials for Vibration Damping, Including Metals, Polymers, Cement and Their Composites. *Journal of Material Science,* Vol. 36, No. 24, pp. 5733-5737, ISSN 0022-2461

Deng, C.F..; Wang,D. Z.; Zhang, X.X. & Ma, Y.X. (2007a). Damping characteristics of carbon nanotube reinforced aluminum composite. *Materials Letters,* Vol.61, pp. 3229–3231, ISSN 0167-577X

Deng, C.F.; Wang, D.Z.; Zhang, X.X. & Li, A.B. (2007b). Processing and properties of carbon nanotubes reinforced aluminum composites. *Materials Science and Engineering A,* Vol.444, pp. 138-145, ISSN 0921-5093

DTA, Handbook on Modal Testing, Dynamic Testing Agency (DTA), 1993

DTA, Primer on Best Practice in Dynamic Testing, Dynamic Testing Agency (DTA), 2000.

Esawi, A. & Morsi, K. (2007). Dispersion of carbon nanotubes (CNTs) in aluminum powder. *Composites A,* Vol.38, pp. 646-650, ISSN 1359-835X

Ewins, D.J. (2001). *Modal Testing: Theory and Practice,* Research Studies Press, 2001, ISBN 0-86380-218-4, London, UK

George, R.; Kashyap, K.T.; Rahul, R. & Yamdagni, S. (2005). Strengthening in carbon nanotube/aluminium (CNT/Al) composites. *Scripta Materialia,* Vol.53, pp. 1159–1163, ISSN 1359-6462

Gi, L.; Ryu, Z.; Jin-Phillipp, N.Y. & Rühle, M. (2006). Investigation of the interfacial reaction between multi-walled carbon nanotubes and aluminum. *Acta Materialia,* Vol.54, pp. 5367-5375, ISSN 1359-6454

Granick, N. & Stem, J.E. (1965). Material Damping of Aluminum by a Resonant Dwell Technique. NASA TN D2893

Gu, J.; Zhang, M.; Gu, M.; Liu, Z. & Zhang, G.; (2004). The damping capacity of aluminum matrix composites reinforced with coated carbon fibers. *Materials Letters,* Vol.58, pp. 3170-3174, ISSN 0167-577X

ICATS Manual, Imperial College Analysis and Testing Software, June 2003.

Imregun, M.; & Ewins, D.J. (1995). Complex modes. - Origin and limits, *Proceedings of 13th IMAC*, pp. 496-506, ISBN 0912053488, Nashville, Tennessee, USA, February 13-16, 1995

Jafari, M.; Enayati, M.H. ; Abbasi, M.H. & Karimzadeh, F. (2009). Thermal stability and structural changes during heat treatment of nanostructured Al2024 alloy. *Journal of Alloys and Compounds,* Vol.478, pp. 260-264, ISSN 0925-8388

Kireitseu, M.; Hui, D. & Tomlinson, G. (2007). Advanced shock-resistant and vibration damping of nanoparticle-reinforced composite material. *Composites: Part B,* Vol.39, No.1, pp. 128-138, ISSN 1359-8368

Koizumi, Y.; Ueyama, M, ; Tsuji, N.; Minamino, Y. & Ota, K. (2003). High Damping Capacity of Ultra-Fine Grained Aluminum Produced by Accumulative Roll Bonding. *Journal of Alloys and Compounds,* Vol. 355, pp. 47-51, ISSN 0925-8388

Srikanth, N. & Gupta, M. (2005). FEM based damping studies of metastable Al/Ti composites. *Journal of Alloys and Compounds,* Vol.394, pp. 226-234, ISSN 0925-8388

Soovere, J. & Drake, M.L. (1985). *Aerospace Structures Technology Damping Design Guide: Technology Review,* Vol 1, AFWALTR- 84-3089, Wright Patterson AFB, OH

Tavoosi, M.; Enayati, M.H. & Karimzadeh, F. (2008). Softening behaviour of nanostructured Al-14wt%Zn alloy during mechanical alloying. *Journal of Alloys and Compounds,* Vol. 464, pp. 107-110, ISSN 0925-8388

Thomson, W.T. (1972). *Theory of Vibration with* Applications, Prentice Hall, ISBN 0-13-651-068-X, Englewood Cliffs, NJ

Williamson, G.K. & Hall, W.H. (1953). *X-ray line broadening from filed aluminium and wolfram. Acta Materialia,* Vol.1, pp. 22-31, ISSN 0412-1961

Yadollahpour, M.; Kadkhodapour, J.; Ziaei-Rad, S. & Karimzadeh, F. (2009). An experimental and numerical investigation on damping capacity of nanocomposite. *Materials Science and Engineering A,* Vol.507, pp. 149-154, ISSN 0921-5093

Zhang, Z. & Zeng, W. (2005). The influence of heat treatment on damping response of AZ91D magnesium alloy. *Materials Science and Engineering A,* Vol.392, pp. 150-155, ISSN 0921-5093
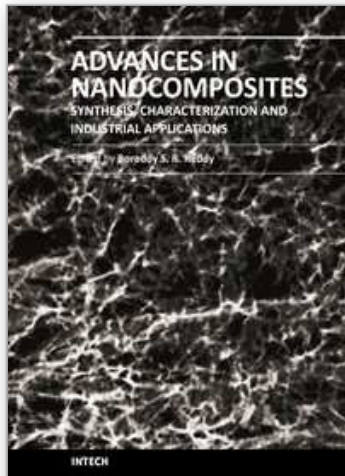
Advances in Nanocomposites - Synthesis, Characterization and Industrial Applications
Edited by Dr. Boreddy Reddy

Advances in Nanocomposites - Synthesis, Characterization and Industrial Applications was conceived as a comprehensive reference volume on various aspects of functional nanocomposites for engineering technologies. The term functional nanocomposites signifies a wide area of polymer/material science and engineering, involving the design, synthesis and study of nanocomposites of increasing structural sophistication and complexity useful for a wide range of chemical, physicochemical and biological/biomedical processes. "Emerging technologies" are also broadly understood to include new technological developments, beginning at the forefront of conventional industrial practices and extending into anticipated and speculative industries of the future. The scope of the present book on nanocomposites and applications extends far beyond emerging technologies. This book presents 40 chapters organized in four parts systematically providing a wealth of new ideas in design, synthesis and study of sophisticated nanocomposite structures.

How to reference

In order to correctly reference this scholarly work, feel free to copy and paste the following:

INTECH
open science | open minds